Biol. Cybern. 77, 453–461 (1997)

Biological Cybernetics

Development of spatiotemporal receptive fields of simple cells: I. Model formulation

S. Wimbauer[1], **O.G. Wenisch**[1], **K.D. Miller**[2], **J.L. van Hemmen**[1]

[1] Physik Department, Technische Universität München, D-85747 Garching, Germany
[2] Departments of Physiology and Otolaryngology, W. M. Keck Foundation Center for Integrative Neuroscience, Sloan Center for Theoretical Neurobiology, University of California, San Francisco, CA 94143-0444, USA

Received: 18 June 1997 / Accepted: 16 September 1997

Abstract. A model for the development of spatiotemporal receptive fields of simple cells in the visual cortex is proposed. The model is based on the 1990 hypothesis of Saul and Humphrey that the convergence of four types of input onto a cortical cell, viz. non-lagged ON and OFF inputs and lagged ON and OFF inputs, underlies the spatial and temporal structure of the receptive fields. It therefore explains both orientation and direction selectivity of simple cells. The response properties of the four types of input are described by the product of linear spatial and temporal response functions. Extending the 1994 model of one of the authors (K.D. Miller), we describe the development of spatiotemporal receptive fields as a Hebbian learning process taking into account not only spatial but also temporal correlations between the different inputs. We derive the correlation functions that drive the development both for the period before and after eye-opening and demonstrate how the joint development of orientation and direction selectivity can be understood in the framework of correlation-based learning. Our investigation is split into two parts that are presented in two papers. In the first, the model for the response properties and for the development of direction-selective receptive fields is presented. In the second paper we present simulation results that are compared with experimental data, and also provide a first analysis of our model.

1 Introduction

Simple cells in the visual cortex of cats and many other mammals represent the first cortical processing stage of the visual pathway. Unlike neurons in the lateral geniculate nucleus (LGN) [27], which project to the visual cortex, most simple cells respond selectively to spatial and temporal stimulus parameters such as orientation [26] or the direction of stimulus motion [28]. The combined spatial and temporal response properties of cortical neurons are summarized by the notion of a spatiotemporal receptive field; for a review see [53].

Correspondence to: J.L. van Hemmen
(e-mail: lvh@physik.tu-muenchen.de)

Since the first discovery of orientation selectivity by Hubel and Wiesel [26], strong efforts have been made to clarify by experimentation the physiological mechanisms that underlie the receptive field properties of simple cells. Much current evidence [7, 18, 21, 54] supports the classical model of Hubel and Wiesel [28] for the origin of orientation selectivity: ON- and OFF-center LGN neurons converge onto a simple cell, forming subregions within the receptive field of the cortical neuron that are aligned along its preferred orientation.

The physiological origins of direction selectivity and other temporal receptive field properties are less clear. There is an ongoing debate on the question of whether direction selectivity is mainly caused by cortico-cortical connections (for a review see [38]) or by geniculo-cortical connections [57]. In either case, direction selectivity might additionally be amplified [14,38] or suppressed [21] by intracortical feedback.

It has been proposed by several authors that a *linear* spatiotemporal receptive field, as can be measured in reverse correlation experiments, might underlie cortical direction selectivity [1,10,12,25,64]. The discovery of non-lagged and lagged cells in the LGN of cats [42, 43] has given support to this hypothesis. Non-lagged and lagged cells that project to the cortex and are combined linearly at a simple cell could provide the temporal offset that is necessary to create a direction-selective receptive field [20, 21, 57]. Experimental support for this hypothesis comes from several sources. In extracellular measurements, an analysis of the time structure of cortical responses shows mixtures of lagged-like and non-lagged-like timing in the responses of direction-selective cells [57]. In intracellular recordings of direction-selective cells [32], analysis of the time structure of excitatory postsynaptic potentials (EPSPs) [34] also demonstrates two underlying temporal components that match the temporal responses of lagged and non-lagged inputs, respectively. Finally, in at least a few cells, direction selectivity emerges in otherwise non-direction-tuned cells when intracortical influences are suppressed, leaving only feed-forward influences [21]. In Sect. 2 we will investigate in greater detail a model of cortical direction selectivity based on convergent lagged and non-lagged input from the LGN. This model will

serve as a working hypothesis throughout this and the following paper.

It is a longstanding view that the development of spatiotemporal receptive field properties of simple cells is governed by an activity-dependent learning process that determines how the synapses are modified during the critical period shortly before and after birth. In the case of orientation selectivity, there is only indirect evidence for this hypothesis. Many simple cells of cats show both orientation and direction selectivity already before eye-opening [3, 5, 29, 52, 58], and monkeys are born with mature orientation selectivity [30]. Thus, it has not been possible to test whether the emergence of orientation selectivity in these species is activity-dependent. In ferrets, the major development of orientation selectivity depends on neural activity, but again some orientation selectivity is present before experimental manipulations of activity are possible [6]. It appears that visual experience cannot substantially modify the preferred orientations of cortical cells [23, 59, 60].[1] In the case of direction selectivity, the evidence for activity-dependent development appears to be stronger: direction selectivity can be abolished by strobe-rearing during the critical period, which abolishes motion from the visual environment, while responsiveness and orientation tuning remain largely intact [4, 31]. Both orientation and direction selectivity are sharpened by normal visual experience; for reviews see [22, 47, 52, 58].

Numerous models have been formulated to describe activity-dependent learning as a self-organization process in accord with a Hebbian rule [16, 17, 35–37, 47, 51, 63, 65, 67]. Most of these models have exclusively concentrated on the development of spatial properties of the receptive field, such as orientation selectivity. In particular, in the model of one of the present authors [16, 47], orientation selectivity develops through a competition between ON-center and OFF-center inputs. The development of orientation selective simple cells is determined mainly by the spatial correlations of the ON- and OFF-cell inputs from the LGN that converge onto the simple cell. The remaining authors of the present paper have developed a framework [65] for extending the spatial correlation-based approach [46, 48] to the learning of spatiotemporal receptive field properties through spatio*temporal* correlations.

In this article, we combine the spatial models of [16, 47] with the spatiotemporal model of [65] to study the joint emergence of direction *and* orientation selectivity through a competition between lagged and non-lagged ON and OFF inputs. A more abstract model that concentrates on the development of direction selectivity alone has concurrently been explored by Feidler et al. [17]. In the same way that the spatial correlation of the input activity plays a key role during the development of orientation selectivity, the temporal correlation of the input activity proves crucial for the development of direction selectivity.

[1] Many early results suggested that a visual environment containing only one orientation would lead to the conversion of all cortical cells to prefer that orientation. However, later work showed that there did not appear to be more than the normal number of cells responsive to that orientation. What had changed was that the number of unresponsive cells increased, presumably because cells that had preferred other orientations were not stimulated and so became "sick" and lost responsiveness [59, 60]. Reviews and discussions of these results can be found in [22, 52, 58].

This paper is organized as follows. In Sect. 2 we introduce the linear model that is used to describe the spatiotemporal response of a simple cell and investigate the context in which such a simple model describes neuronal behavior appropriately. The developmental model itself is then formulated in Sect. 3 and the correlation functions that drive the development are derived both for the period before and after eye-opening.

In a subsequent paper [66] we will present simulation results of our model for different scenarios and compare them with experimental data. Furthermore, a simple analysis of the developmental equation will be performed.

2 Spatiotemporal receptive field properties of simple cells

One of the most accurate experimental methods to measure the structure of spatiotemporal receptive fields of simple cells is the reverse correlation technique [10, 15]. Small bright and dark bars are presented on a dimly lit screen within the receptive field of the cell one records from. From this mesurement one obtains two three-dimensional response profiles, corresponding to bright and dark stimuli, with two spatial dimensions x and y and one temporal dimension t. An (x, y, t) point of such a response profile represents the probability that the cell fires t ms after a small bright or dark bar has been flashed into the cell's receptive field at a position $\boldsymbol{x} = (x, y)$. The spatiotemporal receptive field is obtained by subtracting the two response profiles. The underlying assumption of this subtraction will be discussed later. In a spatiotemporal receptive field, positive values denote bright-excitatory subregions, whereas dark-excitatory subregions are characterized by negative values. In order to facilitate the display of these spatiotemporal receptive fields, one normally integrates along the axis of preferred orientation.

Two types of spatiotemporal receptive fields can be observed experimentally, viz. spatiotemporally separable and non-separable receptive fields [10, 12]. In the first case the response function can be written as the product of a spatial and a temporal part, whereas in the second case this is not possible; for a schematic drawing see Fig. 1a. As was pointed out by Adelson and Bergen [1] and Watson and Ahumada [64], spatiotemporally *non*-separable receptive fields may give rise to a direction-selective response of the cell. An example is shown in Fig. 1b and c. If one assumes that a simple cell acts as a linear spatiotemporal filter, its response to rightward motion can be derived from Fig. 1. A bar oriented along the y-axis (that is perpendicular to the image plane) will evoke its strongest positive response after a longer latency for small x than for large x. If the bar moves to the right at a speed v that corresponds to the slope of the ON subregion in the x-t plane, the difference in latency is compensated for and a short but strong response is evoked at the cell so that the membrane potential will be above the threshold level and the cell will fire. Formally, the response of the cell at a particular time can be obtained from Fig. 1 by integrating along a line of slope v that has its starting point on the lower edge of the receptive field (i.e., where $t = 0$) at the current position of the stimulus. For rightward motion this integration line is parallel to the ON

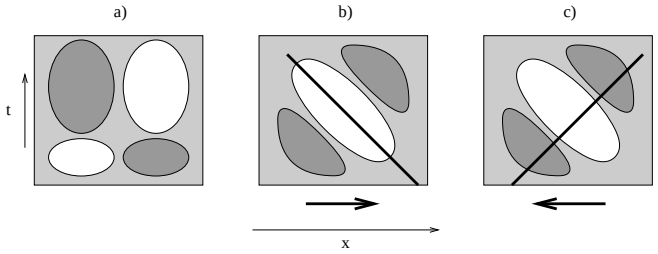

Fig. 1a–c. Spatiotemporal receptive fields for one spatial dimension (axis of motion) and the temporal dimension are displayed schematically. A larger value of t corresponds to a larger time difference between the stimulus and the response, that is, to looking further into the past; cf. the argument of L^τ in (1). **a** A spatiotemporally *separable* receptive field can be described by the product of a spatial and a temporal response function. It responds in the same way to rightward and leftward motion. **b** and **c** A spatiotemporally *non-separable* receptive field that is most sensitive to rightward motion is shown. If a narrow bar oriented perpendicular to the image plane moves along the x-axis at a speed v, the response of the cell at a particular moment can be obtained from the figure by integrating along a line (the thick one) with slope v (towards the t-axis) that cuts the x-axis (where t = 0) at the current position of the stimulus. For a bar moving to the right, the cell response is best if the (thick) integration line runs through the central ON subregion of the spatiotemporal receptive field corresponding to a current position of the stimulus on the right-hand side of the receptive field (cf. **b**). In **c** the stimulus moves to the left. In order to obtain the response of the cell at a particular time one has to integrate along a line of opposite slope to that of **b**. Since the (thick) line now crosses ON and OFF subregions and the sign of the receptive field always varies along such a line, the cell response is weak. For a similar plot cf. [25]

and OFF subregions of the spatiotemporal receptive field and one obtains strong responses when the stimulus crosses the receptive field; cf. Fig. 1b. If the stimulus moves to the left, ON and OFF subregions cancel along the integration line and the cell's response will be weak.

What are the physiological mechanisms that underlie such a spatiotemporal receptive field structure? As was already pointed out in the Introduction, we assume that the convergence of four different types of spatiotemporal channels onto the cortical cell is responsible for the structure of the receptive field. These are ON- and OFF-type channels that come in two different temporal "flavors," namely, non-lagged and lagged. In contrast to the non-lagged channels, the lagged ones show early inhibition rather than excitation. The inhibition is followed by a delayed excitation that is weaker but broader than the initial excitation of non-lagged inputs [57]. The spatiotemporal channels are modeled by the product of a spatial linear response function $R^c(\boldsymbol{\alpha}, \boldsymbol{\alpha}')$ and a temporal one, $L^\tau(t - t', \boldsymbol{\alpha})$, where the index c stands for ON or OFF inputs, the index τ for lagged or non-lagged inputs, and $\boldsymbol{\alpha}$ labels positions in the LGN. The product $R^c(\boldsymbol{\alpha}, \boldsymbol{\alpha}')L^\tau(t-t', \boldsymbol{\alpha})$ describes the response of a cell in the LGN to the activity of the photoreceptors. Such a description is in agreement with the experimental observation that LGN receptive fields are approximately spatiotemporally separable (ignoring the slower temporal response of the surround relative to center) [12]. A spatiotemporal channel characterized by the two functions $R^c(\boldsymbol{\alpha}, \boldsymbol{\alpha}')$ and $L^\tau(t - t', \boldsymbol{\alpha})$ captures LGN responses and thus summarizes processing along the visual pathway from the photoreceptors up to the thalamo-cortical synapse. At the level of the cortex, these channels are summed and weighted by the feed-forward synapses $J^{c,\tau}(\boldsymbol{x}, \boldsymbol{\alpha})$ from the LGN to a simple cell at site $\boldsymbol{x}$ in the visual cortex. A simple cell also receives input from other cortical cells, weighted by intracortical synapses $B(\boldsymbol{x}, \boldsymbol{x}')$. For the sake of simplicity we assume that no additional time structure is introduced by the intracortical connections.

To summarize, we obtain the following functional form for the local potential of a simple cell:

$$h(\boldsymbol{x}, t) = \sum_{c=\text{ON,OFF}} \sum_{\tau=\text{nl,l}} \sum_{\boldsymbol{\alpha}} J^{c,\tau}(\boldsymbol{x}, \boldsymbol{\alpha}) \times \int_{-\infty}^{\infty} d\boldsymbol{\alpha}' \int_{-\infty}^{\infty} dt' R^c(\boldsymbol{\alpha}, \boldsymbol{\alpha}') L^\tau(t - t', \boldsymbol{\alpha}) S(\boldsymbol{\alpha}', t') + \sum_{\boldsymbol{x}'} B(\boldsymbol{x}, \boldsymbol{x}') h(\boldsymbol{x}', t)\,. \quad (1)$$

Here $S(\boldsymbol{\alpha}', t')$ denotes either the deviation of the stimulus intensity from a mean background luminance or the deviation of the photoreceptor activity from a mean noise level at a position $\boldsymbol{\alpha}'$. Therefore, S can take both positive and negative values. For example, during a reverse correlation experiment positive values of S denote a bright bar and negative values a black bar. The coordinate $\boldsymbol{\alpha}$ refers to the retinotopic position of the center of the receptive field of an LGN cell. Finally, $\boldsymbol{x}$ denotes the retinotopic position of a simple cell. It should be noted that the temporal part of the response function may also depend on the retinotopic position of the LGN cell. This is due to our assumption that the main time structure of our model is introduced by non-lagged and lagged cells in the LGN.

Since (1) is linear it can be rewritten

$$h(\boldsymbol{x}, t) = \sum_{\boldsymbol{x}'} I(\boldsymbol{x}, \boldsymbol{x}') \sum_{c=\text{ON,OFF}} \sum_{\tau=\text{nl,l}} \sum_{\boldsymbol{\alpha}} J^{c,\tau}(\boldsymbol{x}', \boldsymbol{\alpha}) \times \int_{-\infty}^{\infty} d\boldsymbol{\alpha}' \int_{-\infty}^{\infty} dt' R^c(\boldsymbol{\alpha}, \boldsymbol{\alpha}') L^\tau(t - t', \boldsymbol{\alpha}) S(\boldsymbol{\alpha}', t') \quad (2)$$

with

$$I(\boldsymbol{x}, \boldsymbol{x}') = \mathbf{1} + B(\boldsymbol{x}, \boldsymbol{x}') + B^2(\boldsymbol{x}, \boldsymbol{x}') + \ldots = [\mathbf{1} - B(\boldsymbol{x}, \boldsymbol{x}')]^{-1}. \quad (3)$$

For the last equation to hold, the eigenvalues of B must have an absolute value of less than one. The spatial kernel $R^c(\boldsymbol{\alpha}, \boldsymbol{\alpha}')$ is supposed to be shift invariant, that is $R^c(\boldsymbol{\alpha}, \boldsymbol{\alpha}') = R^c(\boldsymbol{\alpha} - \boldsymbol{\alpha}')$. The function $R^c(\boldsymbol{\alpha} - \boldsymbol{\alpha}')$ models ON-center and OFF-center receptive fields, and will be given by a Mexican hat function modeled as the difference of two Gaussians [56].

The functional form we have chosen for the temporal linear response function $L^\tau(t-t')$ for a non-lagged or lagged input is based on theoretical considerations due to Dong and Attick [13]. From information-theoretic arguments they were able to derive the following power spectrum of the cell response,

$$L^\tau(\omega) L^\tau(\omega)^* = \frac{\omega^2}{[1 + (\omega/\omega_c)^2]^3}, \quad (4)$$

that agrees well with measurements of Saul and Humphrey [57] for a critical frequency $f_c = \omega_c/(2\pi) \approx 6$ Hz for non-lagged and $f_c \approx 4$ Hz for lagged cells. Because the power spectrum in (4) does not specify the phase of the Fourier

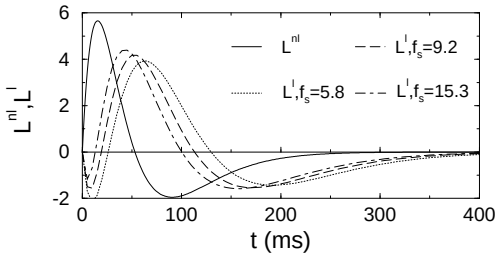

Fig. 2. The non-lagged temporal response function $L^{\mathrm{nl}}(t)$, and lagged response functions $L^{\mathrm{l}}(t)$ for the three values f_s = 5.8, 9.2, and 15.3 Hz, are plotted. The other parameter values are f_c = 6 Hz for non-lagged cells and f_c = 4 Hz for lagged cells. These values have been kept fixed throughout this paper

transform of the response function, it does not determine a unique response function. However, if one imposes the additional constraint that the delay[2] introduced by the filter is minimal [39], one obtains a unique form for the Fourier transform of the temporal response function of non-lagged cells,

$$L^{\mathrm{nl}}(\omega) = \frac{\mathrm{i}\omega}{(1 + \mathrm{i}\omega/\omega_c)^3} \,. \tag{5}$$

For non-lagged cells the requirement of a minimal temporal delay seems to be a plausible assumption on biological grounds. After an inverse Fourier transform the linear response of a non-lagged cell takes the form

$$L^{\mathrm{nl}}(t) = \begin{cases} \frac{1}{N_{\mathrm{nl}}} t(1 - \frac{1}{2}\omega_c t)\mathrm{e}^{-\omega_c t} & \text{for} \quad t \geq 0 \\ 0 & \text{for} \quad t < 0 \end{cases} \tag{6}$$

where the total power of the function L^{nl} is normalized to 1 by the pre-factor $1/N_{\mathrm{nl}}$. Figure 2 shows the response function, which is in good agreement with the linear response function derived experimentally by Saul and Humphrey [57]. The cell fires strongly during the first 50 ms and falls below the mean firing rate for about 300 ms thereafter.

According to measurements recorded by Saul and Humphrey, the response of a lagged channel shows a markedly different form. A short drop in activity is followed by a more delayed and broader peak of the firing rate, as compared to the non-lagged case. The cell activity then falls below the mean firing rate again for another 300 ms. However, the power spectrum of a lagged cell's temporal response is well described by the same function as was found for the non-lagged case.

To obtain the lagged response function, we now, using a purely heuristic approach, multiply the Fourier transform of the non-lagged response function by $(1-\mathrm{i}\omega/\omega_s)/(1+\mathrm{i}\omega/\omega_s)$, to arrive at

$$L^{\mathrm{l}}(\omega) = \frac{\mathrm{i}\omega\,(1 - \mathrm{i}\omega/\omega_s)}{(1 + \mathrm{i}\omega/\omega_c)^3(1 + \mathrm{i}\omega/\omega_s)} \,. \tag{7}$$

In this way the form of the power spectrum (4) that is valid for both non-lagged and lagged cells remains unchanged.[3] The group delay of the response function, however, is increased as compared to the non-lagged one. By varying the shift frequency ω_s, the delay between the lagged and non-lagged response can be tuned. Performing the inverse Fourier transform, one obtains for $t \geq 0$:

$$\begin{aligned} L^{\mathrm{l}}(t) = \mathrm{sgn}(\omega_s - \omega_c)\frac{1}{N_{\mathrm{l}}}\Big\{ & 2\omega_s^2(\mathrm{e}^{-\omega_s t} - \mathrm{e}^{-\omega_c t}) \\ & + \mathrm{e}^{-\omega_c t}\Big[t(\omega_s^3 + \omega_c^3 + \omega_s^2\omega_c - 3\omega_c^2\omega_s) \\ & - \frac{1}{2}t^2\omega_c(\omega_c + \omega_s)(\omega_s - \omega_c)^2\Big]\Big\} \end{aligned} \tag{8}$$

when $\omega_s \neq \omega_c$, and

$$L^{\mathrm{l}}(t) = \frac{1}{N_{\mathrm{l}}} t(-6 + 9\omega_c t - 2\omega_c^2 t^2)\mathrm{e}^{-\omega_c t} \tag{9}$$

when $\omega_s = \omega_c$, while $L^{\mathrm{l}}(t)$ vanishes when $t < 0$.

The functions L^{nl} and L^{l} have been plotted in Fig. 2, showing the form that is to be expected experimentally. The only parameter that has been varied systematically during the simulations is $f_s = \omega_s/(2\pi)$. By changing f_s, the group delay time of the system is modified. It turns out that our model of linear response predicts that, for experimentally observed delays, the correlation between a lagged and a non-lagged channel is very weak.

The question of the degree to which a simple cell's responses can be characterized by a linear spatiotemporal filter has been subject to intense experimental investigation during the last few years. To the degree to which it can be so characterized, it should be possible to predict the response of the cell to a complicated stimulus like a stationary or a drifting sine wave grating from the reverse correlation measurements by simply convolving the input pattern with the spatiotemporal response function. As was shown by DeAngelis et al. [11], tuning curves for spatial and temporal frequency measured with sine-wave gratings agree well with linear predictions from reverse correlation measurements. Furthermore, experiments of Reid et al. [55], Albrecht and Geisler [2] and DeAngelis et al. [11] demonstrate that such a purely linear model accurately evaluates the preferred direction of motion of a simple cell. However, the direction selectivity index, which characterizes the difference in size of the responses for the preferred and the non-preferred direction, is underestimated by a linear model by a factor of 1/3 to 1/2.

It has been proposed by Heeger [25] and by Albrecht and Geisler [2] that a non-linearity describing the spike generation mechanism can account for such discrepancies between the linear model and the experimental results. Membrane potentials are combined linearly in such a model, an idea that is supported by the intracellular recordings of Jagadeesh et al. [32].

One reason for the largely linear behavior of simple cells is that a simple cell is not only excited by a bright stimulus

[2] By delay we mean the group delay of the filter, that is, $\partial\Phi(\omega)/\partial\omega|_{\omega=\omega_0}$ with $\Phi(\omega)$ being the phase of the Fourier transform of the filter and ω_0 being the peak frequency of the Fourier transform of a typical signal. The group delay is a measure for the temporal shift of the envelope of the signal that is introduced by the filter. Besides the requirement of a minimal group delay there are two additional formal requirements so that $L^{\mathrm{nl}}(\omega)$ is defined uniquely by its power spectrum. First, the filter function has to be stable, i.e., $\int_{-\infty}^{+\infty} |L^{\mathrm{nl}}(t)| \exp(-\epsilon|t|)dt < \infty$, and second, it has to be causal, i.e., $L^{\mathrm{nl}}(t) = 0$ for $t < 0$. These two requirements are fulfilled for every "reasonable" filter function

[3] Furthermore, $L^{\mathrm{l}}(\omega)$ is chosen in such a way that it is stable and causal; cf. the previous footnote

presented within the ON subregion of the receptive field, but is also inhibited by a dark stimulus within the ON subregion (and vice versa for OFF subregions) [19]. This makes it reasonable to subtract the spatiotemporal response profiles for a bright and a dark stimulus in a reverse correlation measurement, as described above.

In general, a linear model is always particularly appropriate if only small deviations from a mean value are considered. This is the case in our present study. When we describe the development of the receptive field structure before eye-opening, only small deviations from a mean synaptic strength level are considered, as will be outlined in the next section. Furthermore, the emerging receptive fields are compared with reverse correlation measurements. These predict responses to small deviations from a mean luminance, again justifying the simplicity of our approach.

We now turn to a developmental model that aims to properly incorporate the effects of *time* in the learning equations.

3 A developmental model for spatiotemporal receptive fields

It is commonly assumed that activity-driven modifications of synapses take place according to some sort of Hebbian learning rule [24]. A Hebbian synapse is strengthened if the pre- and postsynaptic activity or depolarization are positively correlated, and is kept fixed or weakened for negative correlations.

A process of long-term potentiation involving NMDA receptors has been proposed [8, 9] as a possible mechanism that might underlie such development by correlated pre- and postsynaptic activity. Sprouting and retraction of axons and dendrites that are guided by neurotrophins could also follow a Hebbian principle, if the amount of neurotrophins available at a certain instant of time and the rate of cell growth are influenced by cell activity [61, 62].

In our model only thalamo-cortical synapses are modified by Hebbian learning, whereas intracortical synapses are kept fixed. Since we aim to describe the development of spatio*temporal* receptive fields we have to carefully consider possible temporal effects in our model. We assume that the change in synaptic strength at time t is determined by the correlation between the postsynaptic membrane potential $h(\boldsymbol{x}, t)$ according to (2) and the presynaptic cell's deviation from a mean firing rate. Then the correlation is integrated over a learning window that lasts for a time Λ so that we find [65]

$$\frac{dJ^{c,\tau}(\boldsymbol{x},\boldsymbol{\alpha},t)}{dt} = \frac{\lambda}{\Lambda}\int_0^{\Lambda} ds A(\boldsymbol{x}-\boldsymbol{\alpha}) h(\boldsymbol{x}, t-s) \tag{10}$$
$$\times\left[\int_{-\infty}^{\infty} dt' \int_{-\infty}^{\infty} d\boldsymbol{\alpha}' R^{c}(\boldsymbol{\alpha}-\boldsymbol{\alpha}') L^{\tau}(t-s-t', \boldsymbol{\alpha}) S(\boldsymbol{\alpha}', t')\right].$$

Here $A(\boldsymbol{x}-\boldsymbol{\alpha})$ denotes an arbor function that restricts the possible synaptic wirings that might emerge from the learning process. In particular, $A(\boldsymbol{x}-\boldsymbol{\alpha})$ indicates the number of synapses between a position $\boldsymbol{\alpha}$ in the LGN and a cortical position $\boldsymbol{x}$ that are modified during development. This mathematical framework can also embrace simple models involving sprouting and retraction guided by a Hebbian principle [50].

In (10) the presynaptic activity is characterized by the full spatiotemporal response function of the channel (nonlagged or lagged) that is linked to the cortical cell by the respective synapse. So the function $L^{\tau}(t, \boldsymbol{\alpha})$ that characterizes the temporal behavior of the different channels appears both in the presynaptic term and the postsynaptic membrane potential. The temporal response properties of the different channels therefore strongly influence the outcome of the learning process.

By inserting (2) into (10) we obtain the following system of differential equations:

$$\frac{dJ^{c,\tau}(\boldsymbol{x},\boldsymbol{\alpha},t)}{dt} = \lambda A(\boldsymbol{x}-\boldsymbol{\alpha}) \sum_{\boldsymbol{x}'} I(\boldsymbol{x},\boldsymbol{x}') \tag{11}$$
$$\times \sum_{c'=\mathrm{ON,OFF}} \sum_{\tau'=\mathrm{nl,l}} \sum_{\boldsymbol{\alpha}'} C^{c,c';\tau,\tau'}(\boldsymbol{\alpha},\boldsymbol{\alpha}',t) J^{c',\tau'}(\boldsymbol{x}',\boldsymbol{\alpha}',t),$$

where $C^{c,c';\tau,\tau'}(\boldsymbol{\alpha},\boldsymbol{\alpha}',t)$ denotes the correlation function

$$C^{c,c';\tau,\tau'}(\boldsymbol{\alpha},\boldsymbol{\alpha}',t) = \int_{-\infty}^{\infty} d\boldsymbol{\alpha}'' \int_{-\infty}^{\infty} d\boldsymbol{\alpha}''' R^{c}(\boldsymbol{\alpha}-\boldsymbol{\alpha}'') R^{c'}(\boldsymbol{\alpha}'-\boldsymbol{\alpha}''')$$
$$\times \int_{-\infty}^{\infty} dt' \int_{-\infty}^{\infty} dt'' L^{\tau}(t-t', \boldsymbol{\alpha}) L^{\tau'}(t-t'', \boldsymbol{\alpha}')$$
$$\times \frac{1}{\Lambda}\int_0^{\Lambda} ds S(\boldsymbol{\alpha}'', t'-s) S(\boldsymbol{\alpha}''', t''-s). \tag{12}$$

In (11) and (12) we have made the additional assumption that $J^{c,\tau}(\boldsymbol{x},\boldsymbol{\alpha},t)$ changes slowly within the timescale of the learning window. In particular, we set $J^{c,\tau}(\boldsymbol{x},\boldsymbol{\alpha},t)$ constant within the learning window so that a separation of timescales is performed.

The term $1/\Lambda \int_0^{\Lambda} ds S(\boldsymbol{\alpha}'', t'-s) S(\boldsymbol{\alpha}''', t''-s)$ describes the correlation of the activity of the photoreceptors in space and time, averaged over a learning period Λ. We now consider two possible cases that might be crucial for the development of direction selectivity, and their corresponding correlation functions. In the first case uncorrelated noise in the photoreceptors drives the development, whereas in the second case development in an environment of moving gratings is considered.

Orientation and direction selectivity already develop before eye-opening [3, 29, 52, 58]. Correlations within the input activity $S(\boldsymbol{\alpha}, t)$ during this period result from noise in the photoreceptors. One plausible assumption, and also the simplest one, is that a photoreceptor's deviation from the mean noise level is uncorrelated in space and time and fluctuates fast as compared to the time period Λ. This gives:

$$\frac{1}{\Lambda}\int_0^{\Lambda} ds S(\boldsymbol{\alpha}'', t'-s) S(\boldsymbol{\alpha}''', t''-s) = \delta(\boldsymbol{\alpha}'''-\boldsymbol{\alpha}'', t''-t'). \tag{13}$$

Using (13), the expression for the correlation function (12) simplifies considerably, and we obtain

$$C^{c,c';\tau,\tau'}(\boldsymbol{\alpha},\boldsymbol{\alpha}',t) = C^{c,c'}(\boldsymbol{\alpha},\boldsymbol{\alpha}') C^{\tau,\tau'}(\boldsymbol{\alpha},\boldsymbol{\alpha}') \tag{14}$$

with

$$C^{c,c'}(\boldsymbol{\alpha},\boldsymbol{\alpha}') = \int_{-\infty}^{\infty} d\boldsymbol{\alpha}'' R^{c}(\alpha-\alpha'') R^{c'}(\alpha'-\alpha''), \tag{15}$$

$$C^{\tau,\tau'}(\boldsymbol{\alpha},\boldsymbol{\alpha}') = \int_{-\infty}^{\infty} dt L^{\tau}(t,\boldsymbol{\alpha}) L^{\tau'}(t,\boldsymbol{\alpha}'). \tag{16}$$

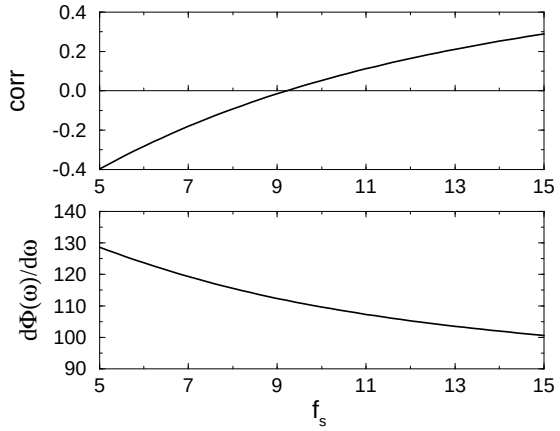

Fig. 3. The temporal correlation between non-lagged and lagged inputs corr(f_s) and the group delay time $\partial\Phi(\omega)/\partial\omega|_{\omega=\omega_{\rm opt}}$ of the lagged response function (in ms), for $\omega_{\rm opt} \approx 2\pi \times 2.8$ Hz (approximate peak of the power spectrum), have been plotted as a function of f_s

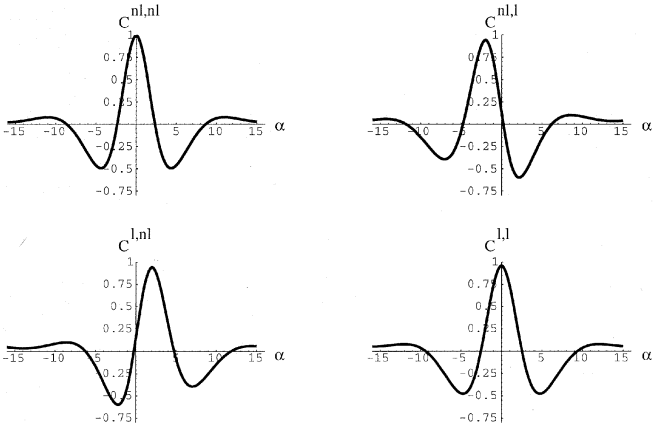

Fig. 4. The four correlation functions corresponding to different combinations of non-lagged and lagged inputs are displayed for the case of a narrow bar of light moving from left to right across the retina at a speed of 15°/s. The whole receptive field has a width of 3°. It should be noted that the correlation function is no longer rotationally symmetric as in the case of unstructured input; cf. (17). Along the α-axis one finds strong oscillations, as shown; these oscillations are smoother along the β-axis, perpendicular to the picture plane, so that excursions to negative values are small or totally missing along that axis. Note that the peaks of $C^{\rm l,nl}(\boldsymbol{\alpha}-\boldsymbol{\alpha}')$ and $C^{\rm nl,l}(\boldsymbol{\alpha}-\boldsymbol{\alpha}')$ are shifted in or opposite to the direction of motion, in contrast to the central peaks of $C^{\rm nl,nl}(\boldsymbol{\alpha}-\boldsymbol{\alpha}')$ and $C^{\rm l,l}(\boldsymbol{\alpha}-\boldsymbol{\alpha}')$

The spatial part of the correlation function $C^{c,c'}(\boldsymbol{\alpha},\boldsymbol{\alpha}')$ is given by the convolution of two center-surround receptive fields and gives a Mexican-hat-type correlation function, as has already been pointed out by Miller [47]. For the sake of simplicity we model this correlation function as the difference of two Gaussians:

$$C^{\rm ON,ON}(\boldsymbol{\alpha},\boldsymbol{\alpha}') = C^{\rm OFF,OFF}(\boldsymbol{\alpha},\boldsymbol{\alpha}') = \exp\left(-\frac{|\boldsymbol{\alpha}-\boldsymbol{\alpha}'|^2}{\sigma_c^2}\right) - \frac{1}{\gamma_c^2}\exp\left(-\frac{|\boldsymbol{\alpha}-\boldsymbol{\alpha}'|^2}{\gamma_c^2\sigma_c^2}\right). \quad (17)$$

Furthermore, if $R^{\rm ON}(\boldsymbol{\alpha},\boldsymbol{\alpha}') = -R^{\rm OFF}(\boldsymbol{\alpha},\boldsymbol{\alpha}')$ it follows that

$$C^{\rm ON,OFF}(\boldsymbol{\alpha},\boldsymbol{\alpha}') = C^{\rm OFF,ON}(\boldsymbol{\alpha},\boldsymbol{\alpha}') = -C^{\rm ON,ON}(\boldsymbol{\alpha},\boldsymbol{\alpha}')\,. \quad (18)$$

We have also performed simulations with $C^{\rm ON,OFF} = C^{\rm OFF,ON} = -0.5\,C^{\rm ON,ON}$, as used in most simulations of Miller [47]. The structure of the simulation results, however, has not been affected by this change of the correlation function.

According to (16), the temporal part of the correlation function $C^{\tau,\tau'}(\boldsymbol{\alpha},\boldsymbol{\alpha}')$ depends on the functional form of the temporal response function. In most of the simulations described in the following article [66] we make the simplifying assumption that $L^{\tau}(t,\boldsymbol{\alpha})$ does not depend on the position $\boldsymbol{\alpha}$ of the LGN neuron. Then $C^{\tau,\tau'}(\boldsymbol{\alpha},\boldsymbol{\alpha}')$ reduces to the 2×2 matrix

$$C^{\tau,\tau'} = \begin{pmatrix} C^{\rm nl,nl} & C^{\rm nl,l} \\ C^{\rm l,nl} & C^{\rm l,l} \end{pmatrix} = \begin{pmatrix} 1 & {\rm corr} \\ {\rm corr} & 1 \end{pmatrix}. \quad (19)$$

The diagonal elements are 1 because of the normalization of the temporal response functions. The only parameter that will be varied systematically during the simulations presented in [66] is f_s. It determines the form of the lagged response function and, in particular, the group delay time of the filter. Hence we obtain

$${\rm corr}(f_s) = \int_{-\infty}^{\infty} dt L^{\rm nl}(t)L^{\rm l}(t,f_s)\,. \quad (20)$$

The dependence of the function corr(f_s) upon f_s and the group delay time of a lagged response function have been plotted in Fig. 3. The group delay time is given by $\partial\Phi(\omega)/\partial\omega|_{\omega=\omega_{\rm opt}}$ where $\Phi(\omega)$ is the phase of the Fourier transform of the lagged response function $L^{\rm l}(\omega)$ and $\omega_{\rm opt} \approx 2\pi\times 2.8$ Hz denotes the frequency where the power spectrum of the response of a lagged cell has its maximum.

If we vary f_s between 5 and 15 Hz, the passage time varies between 130 and 100 ms, which are typical delays for lagged cells according to Saul and Humphrey [57]. The function corr(f_s), on the other hand, increases from -0.4 to 0.3 and vanishes when f_s = 9.2 Hz.

It will turn out that for corr(f_s) near zero, that is, for weak correlations between lagged and non-lagged cells, strongly direction-selective receptive fields emerge, as observed experimentally.

We now turn to a second case and derive the correlation function that corresponds to an environment of moving gratings. Such a structured input might arise either from patterned vision after eye-opening or from spindle waves traversing the LGN during sleep [33, 44].

For simplicity we consider an infinitely narrow line/bar that moves into the α-direction at a speed v. For this case the activity of a photoreceptor at time t' and at point α'' is correlated with the activity of the photoreceptor at time t'' and at point $\alpha''' = \alpha'' + (t''-t')v$, since the bar has moved from α'' to α''' during the time interval $t''-t'$. Hence, the correlation of the activity of the photoreceptors takes the form

$$\frac{1}{\Lambda}\int_0^{\Lambda} ds S(\boldsymbol{\alpha}'',t'-s)S(\boldsymbol{\alpha}''',t''-s) = \delta(\alpha'''-\alpha''-(t''-t')v) \quad (21)$$

where $\boldsymbol{\alpha} = (\alpha,\beta)$.

Inserting (21) into (12) and performing the integration in (12) one obtains complicated functional forms for the four spatial correlation functions corresponding to the different combinations of non-lagged and lagged inputs. We do not describe these functions explicitly but display them in Fig. 4

for the case of $v = 15°$/s and a width of a receptive field of about 3°. While $C^{\mathrm{nl,nl}}(\boldsymbol{\alpha}, \boldsymbol{\alpha}')$ and $C^{\mathrm{l,l}}(\boldsymbol{\alpha}, \boldsymbol{\alpha}')$ have a central peak, the maximum of $C^{\mathrm{nl,l}}(\boldsymbol{\alpha}, \boldsymbol{\alpha}')$ and $C^{\mathrm{l,nl}}(\boldsymbol{\alpha}, \boldsymbol{\alpha}')$ is shifted in or opposite to the direction of motion.

The general case of bars with different directions of motion is either modeled by averaging the correlation function in Fig. 4 over different directions of motion or by rotating the correlation function during a simulation run.

We would like to stress that our approach of deriving the correlation functions from a model of linear response for the different channels can only serve as a kind of plausible argument for the form of the correlation functions. It would be more desirable to obtain these functions directly from cross-correlation measurements in the LGN. There exist some experimental data about the correlations in activity between retinal ganglion cells [40,41,45] that are consistent with the form of the spatial correlation function as given in (17). However, data on temporal correlations between non-lagged and lagged cells in the LGN are not available yet.

The arbor function $A(\boldsymbol{x}-\boldsymbol{\alpha})$ and the intracortical interaction function $I(\boldsymbol{x}-\boldsymbol{x}')$ have been chosen in agreement with Miller [47]. Here $A(\boldsymbol{x}-\boldsymbol{\alpha})$ is proportional to the overlap in area of a circle of radius r_A and a circle of radius $c_A r_A$ with centers separated by $|\boldsymbol{x}-\boldsymbol{\alpha}|$. It is zero for $|\boldsymbol{x}-\boldsymbol{\alpha}| > D_A/2$, where D_A is the arbor diameter, with $r_A = (D_A - 1)/2$ and $c_A = 0.5$. The function $I(\boldsymbol{x} - \boldsymbol{x}')$ is a Mexican hat of the form

$$I(\boldsymbol{x}) = a(\boldsymbol{x}) \left[\exp\left(-\frac{|\boldsymbol{x}|^2}{\sigma_I^2} \right) - \frac{1}{\gamma_I^2} \exp\left(-\frac{|\boldsymbol{x}|^2}{\gamma_I^2 \sigma_I^2} \right) \right] . \qquad (22)$$

As mentioned above only the parameter f_s that determines the form of the lagged response is varied systematically in the simulations described in the second paper [66]. The other parameters have been chosen in such a way [47] that stable orientation selectivity emerges for the purely spatial case. In particular, for the case of a noise-driven development we assign the values $\sigma_c = r_c D_A/2$ with $r_c = 0.25$ and $\gamma_c = 3$ to the parameters of the spatial correlation function. For the scenario in which moving gratings determine the development we choose a speed of $v = 15°$/s for the patterns moving across the retina. Furthermore, we have taken for the parameters of the intracortical interaction function the values $\sigma_I = r_I D_A/2$ with $r_I = 0.25$ or $r_I = 0.4$, $\gamma_I = 3$, and $a(0)$=1 for $\boldsymbol{x} = 0$ and $a(\boldsymbol{x}) = 0.5$ otherwise. So the width of both the correlation function and the intracortical interaction function scale with the diameter of the arbor function. For a more detailed discussion of the different parameter values see Miller [47].

If synapses are modified according to (11), they will grow or decrease boundlessly [49]. To avoid such biologically implausible behavior, upper and lower limits of the couplings have been introduced. Since all afferent thalamocortical couplings are assumed to be excitatory, we set

$$0 \le J^{c,\tau}(\boldsymbol{x}, \boldsymbol{\alpha}) \le J_{\max} A(\boldsymbol{x} - \boldsymbol{\alpha}) \qquad (23)$$

with a default value $J_{\max} = 4$. Moreover, (11) is completed by a constraint that ensures that the sum of the synaptic weights received by one cortical cell is kept fixed. In this way a competitive process between afferent axons is modeled.

The full learning equation then takes the form

$$\begin{aligned} \frac{dJ^{c,\tau}(\boldsymbol{x}, \boldsymbol{\alpha}, t)}{dt} &= \lambda A(\boldsymbol{x} - \boldsymbol{\alpha}) \sum_{\boldsymbol{x}'} I(\boldsymbol{x}, \boldsymbol{x}') \\ &\quad \times \sum_{c'} \sum_{\tau'} \sum_{\boldsymbol{\alpha}''} C^{c,c';\tau,\tau'}(\boldsymbol{\alpha}, \boldsymbol{\alpha}'') J^{c',\tau'}(\boldsymbol{x}', \boldsymbol{\alpha}'', t) \\ &\quad - \epsilon(\boldsymbol{x}) A(\boldsymbol{x} - \boldsymbol{\alpha}), \end{aligned} \qquad (24)$$

where

$$\epsilon(\boldsymbol{x}) = \frac{\left[\sum_{\boldsymbol{\alpha}'} \sum_{c=\mathrm{ON,OFF}} \sum_{\tau=\mathrm{nl,l}} \frac{d}{dt}\Big|_{\mathrm{u}} J^{c,\tau}(\boldsymbol{x}, \boldsymbol{\alpha}', t) \right]}{\sum_{\boldsymbol{\alpha}',c,\tau} A^{c,\tau}(\boldsymbol{x} - \boldsymbol{\alpha}')} \qquad (25)$$

and $\frac{d}{dt}\big|_{\mathrm{u}} J^{c,\tau}(\boldsymbol{x}, \boldsymbol{\alpha}')$ is given by (11). Here $A^{c',\tau'}(\boldsymbol{x}-\boldsymbol{\alpha}'') = A(\boldsymbol{x} - \boldsymbol{\alpha})$ for all c' and τ' (the arbor function is identical for all input types); explicitly noting the input type will be useful when we consider inactivation of synapses that reach the maximum or minimum allowed values. The effects of the constraint on the dynamics of the learning equation have been discussed in detail elsewhere [49].

4 Outlook

In a subsequent paper [66] we study the developmental model derived above in numerical simulations and present a first analysis of the model. We consider different scenarios that cover the development both before and after eye-opening. A thorough discussion of our model and a comparison with experimental data will also be presented there.

References

1. Adelson EH, Bergen JR (1985) Spatiotemporal energy models for the perception of motion. J Opt Soc Am A 2:284–299
2. Albrecht DG, Geisler WS (1991) Motion selectivity and the contrast response function of simple cells in the visual cortex. Vis Neurosci 7:531–546
3. Albus K, Wolf W (1984) Early post-natal development of neuronal function in the kitten's visual cortex: a laminar analysis. J Physiol (Lond) 348:153–185
4. Blakemore C, Sluyters RC van (1975) Innate and environmental factors in the development of the kitten's visual cortex. J Physiol (Lond) 248:663–716
5. Braastadt BO, Heggelund P (1985) Development of spatial receptive-field organization and orientation selectivity in kitten striate cortex. J Neurophysiol 53:1158–1178
6. Chapman B, Stryker MP (1993) Development of orientation selectivity in ferret visual cortex and effects of deprivation. J Neurosci 13:5251–5262
7. Chapman B, Zahs KR, Stryker MP (1991) Relation of cortical cell orientation selectivity to alignment of receptive fields of the geniculocoritcal afferents that arborize within a single orientation column in ferret visual cortex. J Neurosci 11:1347–1358
8. Constantine-Paton M, Cline HT, Debski E (1990) Patterned activity, synaptic convergence, and the NMDA receptor in developing visual pathways. Annu Rev Neurosci 13:129–154
9. Crair MC, Malenka RC (1995) A critical period for long-term potentiation at thalamocortical synapses. Nature 375:325–328
10. DeAngelis GC, Ohzawa I, Freeman RD (1993) Spatiotemporal organization of simple-cell receptive fields in the cat's striate cortex. I. General characteristics and postnatal development. J Neurophysiol 69:1091–1117

11. DeAngelis GC, Ohzawa I, Freeman RD (1993) Spatiotemporal organization of simple-cell receptive fields in the cat's striate cortex. II. linearity of temporal and spatial summation. J Neurophysiol 69:1118–1135
12. DeAngelis GC, Ohzawa I, Freeman RD (1995) Receptive-field dynamics in the central visual pathways. Trends Neurol Sci 18:451–458
13. Dong DW, Atick JJ (1995) Temporal decorrelation: a theory of lagged and nonlagged responses in the lateral geniculate nucleus. Network 6:159–178
14. Douglas RJ, Koch C, Mahowald M, Martin KAC, Suarez HH (1995) Recurrent excitation in neocortical circuits. Science 269:981–985
15. Eckhorn R, Krause F, Nelson JI (1993) The RF-cinematogram: a cross-correlation technique for mapping several visual fields at once. Biol Cybern 69:37–55
16. Erwin E, Miller KD (1996) Modeling joint development of ocular dominance and orientation maps in primary visual cortex. In: Bower JM (ed) Computational neuroscience: trends in research 1995. Academic Press, New York, pp 179–184 Available as ftp://ftp.keck.ucsf.edu/pub/erwin/CNS95proc.ps.Z.
17. Feidler JC, Saul AB, Murthy A, Humphrey AL (1997) Hebbian learning and the development of direction selectivity: the role of geniculate response timings. Network 8:195–214
18. Ferster D (1987) Origin of orientation-selective EPSPs in simple cells of cat visual cortex. J Neurosci 7:1780–1791
19. Ferster D (1988) Spatially opponent excitation and inhibition in simple cells of the cat visual cortex. J Neurosci 8:1172–1180
20. Ferster D (1994) Linearity of synaptic interactions in the assembly of receptive fields in cat visual cortex. Curr Opin Neurobiol 4:563–568
21. Ferster D, Chung S, Wheat H (1996) Orientation selectivity of thalamic input to simple cells of cat visual cortex. Nature 380:249–252
22. Fregnac Y, Imbert M (1984) Development of neuronal selectivity in the primary visual cortex of cat. Physiol Rev 64:325–434
23. Gödecke I, Bonhoeffer T (1996) Development of identical orientation maps for two eyes without common visual experience. Nature 379:251–254
24. Hebb DO (1949) The organization of behavior. Wiley, New York
25. Heeger DJ (1993) Modelling simple-cell direction selectivity with normalized, half-squared, linear operators. J Neurophysiol 70:1885–1898
26. Hubel DH, Wiesel TN (1959) Receptive fields of single neurons in the cat's striate cortex. J Physiol (Lond) 148:574–591
27. Hubel DH, Wiesel TN (1961) Integrative action in the cat's lateral geniculate body. J Physiol (Lond) 155:385–398
28. Hubel DH, Wiesel TN (1962) Receptive fields, binocular interaction and functional architecture in the cat's visual cortex. J Physiol (Lond) 160:106–154
29. Hubel DH, Wiesel TN (1963) Receptive fields of cells in striate cortex of very young, visually inexperienced kittens. J Neurophysiol 26:994–1002
30. Hubel DH, Wiesel TN (1974) Uniformity of monkey striate cortex: a parallel relationship between field size, scatter and magnification factor. J Comp Neurol 158:295–306
31. Humphrey AL, Saul AB (1995) Strobe rearing alters the spatiotemporal structure of simple cell receptive fields in cat area 17. Soc Neurosci Abstr 21:1648
32. Jagadeesh B, Wheat HS, Ferster D (1993) Linearity of summation of synaptic potentials underlying direction selectivity in simple cells of the cat visual cortex. Science 262:1901–1904
33. Kim U, Bal T, McCormick DA (1995) Spindle waves are propagating synchronized oscillations in the ferret LGNd in vitro. J Neurophysiol 74:1301–1323
34. Kontsevich LL, Tyler CW, Ferster D (1995) Synaptic inputs underlying direction selectivity in simple cells of the cat visual cortex. Preprint
35. Linsker R (1986) From basic network principles to neural architecture: emergence of orientation selective cells. Proc Natl Acad Sci USA 83:8390–8394
36. Linsker R (1986) From basic network principles to neural architecture: emergence of orientation columns. Proc Natl Acad Sci USA 83:8779–8783
37. Linsker R (1986) From basic network principles to neural architecture: emergence of spatial-opponent cells. Proc Natl Acad Sci USA 83:7508–7512
38. Maex R (1994) Direction-selective simple cells in cat striate cortex: a modelling study. Leuven University Press, Leuven
39. Marko H (1986) Methoden der Systemtheorie. Springer, Berlin Heidelberg New York
40. Mastronarde DN (1983) Correlated firing of cat retinal ganglion cells. I. Spontaneously active inputs to X and Y cells. J Neurophysiol 49:303–324
41. Mastronarde DN (1983) Correlated firing of cat retinal ganglion cells. II. Responses of X- and Y-cells to single quantal events. J Neurophysiol 49:325–349
42. Mastronarde DN (1987) Two classes of single-input X cells in cat lateral geniculate nucleus. I. Receptive-field properties and classification of cells. J Neurophysiol 57:357–380
43. Mastronarde DN (1987) Two classes of single-input X cells in cat lateral geniculate nucleus. II. Retinal inputs and the generation of receptive field properties. J Neurophysiol 57:381–413
44. McCormick DA, Trent F, Ramoa AS (1995) Postnatal development of synchronized network oscillations in the ferret dorsal lateral geniculate and perigeniculate nuclei. J Neurosci 15:5739–5752
45. Meister M, Lagnado L, Baylor DA (1995) Concerted signaling by retinal ganglion cells. Science 270:1207–1210
46. Miller KD (1990) Derivation of linear Hebbian equations from a nonlinear Hebbian model of synaptic plasticity. Neural Comput 2:321–333
47. Miller KD (1994) A model for the development of simple cell receptive fields and the ordered arrangement of orientation columns through activity dependent competition between ON- and OFF-center inputs. J Neurosci 14:409–441
48. Miller KD (1995) Receptive fields and maps in the visual cortex: Models of ocular dominance and orientation columns. In: Domany E, Hemmen LL van, Schulten K (eds) Models of neural networks III. Springer, New York Berlin Heidelberg, pp 55–78
49. Miller KD, MacKay DJC (1994) The role of constraints in Hebbian learning. Neural Comput 6:100–126
50. Miller KD (1997) Equivalence of a sprouting–and–retraction model and correlation–based plasticity models of neural development. Neural Comput (in press)
51. Miller KD, Keller JB, Stryker MP (1989) Ocular dominance column development: Analysis and simulation. Science 245:605–615
52. Movshon JA, Sluyters RC van (1981) Visual neural development. Annu Rev Psychol 32:477–522
53. Orban GA (1991) The neural basis of visual function. In: Leventhal AG (ed) Quantitative electrophysiology of visual cortical neurons, vol 4. CRC Press, Boca Raton, pp 173–222.
54. Reid RC, Alonso J (1995) Specificity of monosynaptic connections from thalamus to visual cortex. Nature 378:281–284
55. Reid RC, Soodak RE, Shapley RM (1991) Directional selectivity and spatiotemporal structure of receptive fields of simple cells in cat striate cortex. J Neurophysiol 66:505–529
56. Rodieck RW (1965) Quantitative analysis of cat retinal ganglion cell response to visual stimuli. Vis Res 5:583–601
57. Saul AB, Humphrey AL (1990) Spatial and temporal response properties of lagged and nonlagged cells in cat lateral geniculate nucleus. J Neurophysiol 64:206–224
58. Sherman SM, Spear PD (1982) Organization of visual pathways in normal and visually deprived cats. Physiol Rev 62:738–855
59. Stryker MP, Sherk H (1975) Modification of cortical orientation selectivity in the cat by restricted visual experience: a reexamination. Science 190:904–906
60. Stryker MP, Sherk H, Leventhal AG, Hirsch VB (1978) Physiological consequences for the cat's visual cortex of effectively resticting early visual experience with oriented contours. J Neurophysiol 41:896–909
61. Thoenen H (1995) Neurotrophins and neuronal plasticity. Science 270:593–598
62. Ooyen A van Activity-dependent neural network development. Network 5:401–423
63. Malsburg C von der (1973) Self-organization of orientation selective cells in the striate cortex. Kybernetik 14:85–100
64. Watson AB, Ahumada AJ (1985) Model of human visual motion sensing. J Opt Soc Am A 2:322–342
65. Wimbauer S, Gerstner W, Hemmen JL van (1994) Emergence of

spatiotemporal receptive fields and its application to motion detection. Biol Cybern 72:81–92
66. Wimbauer S, Wenisch OG, Miller KD, Hemmen JL van (1997) Development of spatiotemporal receptive fields of simple cells: II. Simulation and analysis. Biol Cybern 77:463–477
67. Yuille AL, Kammen DM, Cohen DS (1989) Quadrature and the development of orientation selective cortical cells by Hebb rules. Biol Cybern 61:183–194